Nagua,L., Monje, C. A., Muñóz, J. y Balaguer, C. (2018). Design and performance validation of a cable-driven soft robotic neck. In *Jornadas Nacionales de Robótica*, JNR 2018, pp. 1-6.

Jornadas Nacionales de Robótica
Spanish Robotics Conference
14-15 Junio 2018 http://jnr2018.eii.uva.es

Design and performance validation of a cable-driven soft robotic neck

Luis Nagua[1], Concepción A. Monje[1], Jorge Muñoz[1], Carlos Balaguer[1]

Robotics Lab, Departmento de Ingeniería de Sistemas y Automática, Universidad Carlos III de Madrid, Avda. de la Universidad 30, 28911 Leganés, España

Abstract

The purpose of this paper is to design a soft robotic neck prototype with two Degrees of Freedom (DOF). It is mainly aimed to investigate, study and design a mechanism that allows to simulate the movements of a human neck, concretely the movements of flexion, extension and lateral bending. To archieve these movements, the design is made based on a cable-driven mechanism, validating the design of spring, through which it will be possible to obtain the sketch of the components that make up the soft neck and then its manufacture in a 3D printer. Another important aspect for the development of the project is the load weight that the soft neck can support, in order to size the motors that are needed for the operation of the parallel mechanism. In addition, the analysis of its mathematical model for the control system that will be implemented in future work is carried out.

Keywords:
Cable-Driven Parallel Mechanisms (CDPM), Soft robotics, Neck prototype, Design and modelling.
Datos del Proyecto:
Denominación del proyecto: HUMASoft
Referencia: DPI2016-75330-P
Investigador/es responsable/es: Concepción Alicia Monje Micharet
Tipo de proyecto (internacional, nacional, autonómico, transferencia): Nacional
Entidad/es financiadora/s: Ministerio de Economía y Competitividad
Fecha de inicio/fin: 2016/2019
Alternativamente:
Datos de la tesis: Diseño y Control de Eslabones Blandos para Robots Humanoides.
Doctorando: Luis Nagua Cuenca
Directores: Concepción Alicia Monje Micharet
Fecha Inicio/Fecha estimada terminación: 04-2018/04-2021
Programa de doctorado: Ingeniería Eléctrica, Electrónica y Automática
Universidad: Universidad Carlos III de Madrid

1. Introduction

Nowadays, there exists a new trend on biologically inspired robots with "soft" elements that are able to perform tasks which are not available to robots with rigid limbs. In the case of humanoid robotics, a robot with soft links has the following main advantages: a) simplicity of design, favouring an underactuated architecture; b) accessibility and adaptability to complex environments; and c) safer interaction with the human and the environment.

Focusing on the neck element, there are several humanoid neck mechanisms developed by different researchers. They can be divided into two categories, i.e. serial necks and parallel necks.

The neck in series is very used due to its easy control, since each DOF of the neck is operated independently. Robotic necks in series such as HRP-4 (Hirukawa et al. (2004)) and Honda ASIMO-2002 (Sakagami et al. (2002)) have two DOF (pitch, yaw). The four-bar robotic neck in (Tadesse et al. (2010)) also has two DOF. There are also designs with tree DOF, for example Albert HUBO (Tadesse et al. (2010)), Dav (Han et al. (2002)) and the final design of iCub (Beira et al. (2006)).

Parallel robot necks are based in general on a parallel manipulator, which consists of a mobile platform, a fixed base, several identical active chains and a passive backbone, if necessary. This type of mechanism is interesting for the following reasons: the number of actuators is minimal, the number of sensors necessary for the closed-loop control of the mechanism is minimal. when the actuators are locked, the manipulator remains in its position; this is an important safety aspect for certain applications, such as medical robotics. The parallel mechanism in (Gao et al. (2011)) has four conductor cables and performs two DOF of a human neck (pitch, roll). The SAYA head has a structure composed of a central spring and several pneumatic artificial

Email addresses: `lnagua@ing.uc3m.es` (Luis Nagua), `cmonje@ing.uc3m.es` (Concepción A. Monje), `jmyanezb@ing.uc3m.es` (Jorge Muñoz), `balaguer@ing.uc3m.es` (Carlos Balaguer)

[1]Robotics Lab of the Carlos III University of Madrid, Avda de la Universidad 30, 28911 Leganés, Madrid, Spain

muscles(Hashimoto et al. (2006)).

Cable-based robots have several advantages (Behzadipour y Khajepour (2006)) over the conventional mechanisms of rigid joints in series or parallel, which include: large workspace, low inertia and a significant simplification of the mechanical transmission design.

In this paper a soft robotic cable-driven mechanism is proposed with the purpose of later creating softer humanoid robots that meet the characteristics of simplicity, accessibility and safety. It is the purpose for this soft link to be used interchangeably in various limbs of the humanoid robot, like arms, neck and spine, under the constraints of scalability, controllability of their stiffness and integration. The first step towards this goal is the design and performance analysis of a prototype of soft link working as a neck, with definition of its material and its actuation system.

The paper is organized as follows: Section 2 presents the mechanical and electrical design of the mechanism. Section 3 introduces the mathematical analysis of the reverse kinematics and lateral buckling of the spring, and Section 4 performs the validation of the spring design. Finally, Section 5 outlines the main conclusions of the paper.

2. Desing of the prototype

The prototype proposed in this paper is the result of research on robot necks, mainly in the configuration of parallel robots for the advantages of (Behzadipour y Khajepour (2006)). The motions of the human neck include flexion / extension (pitch), vertical rotation (yaw) and lateral flexion (roll) (Alfayad et al. (2016)), as shown in Fig. 1. The flexion movement with a range of 50°, while the extension has a range of 57.5°, ensures that the head is tilted backwards. The vertical rotation of the neck is described as the rotation of the head to the right and to the left with a rotation range of 70 °. The lateral flexion allows the head to bend towards the shoulder, with a maximum angle of 45°.

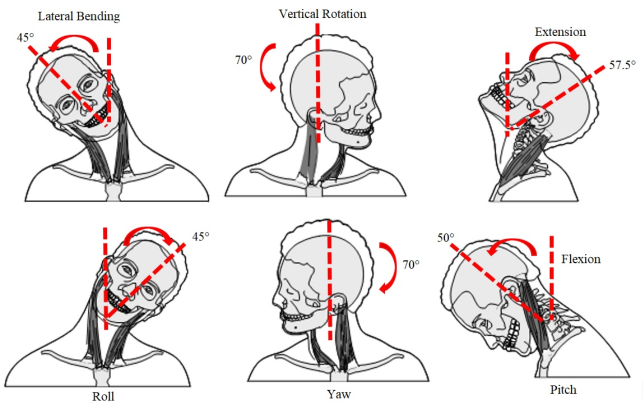

Figure 1: Human neck motions.

The purpose of this paper is to design a soft robotic neck of two DOF (pitch and roll) with a maximum tilt angle of 40°, under a criterion of flexibility and inspired by the human neck structure, using a column spring. The mechanism will support a load of $1Kg$.

The design of the prototype includes the four steps shown in Fig. 2: selection of the cable-driven parallel mechanism, design of the mechanical system, requirements of the electrical system and design of the overall soft neck prototype. All these stages will be described in detail in the following sections.

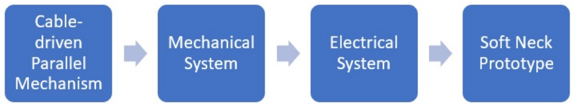

Figure 2: Steps for prototype design.

2.1. *Cable-Driven Parallel Mechanism (CDPM)*

Parallel robots for which the number of chains is strictly equal to the number of DOF of the end-effector are called fully parallel manipulators. Gosselin (Gosselin (June, 15, 1988)) characterizes fully parallel manipulators by the equation:

$$p(n-6) = -6 \tag{1}$$

where p represents the number of DOF and n the number of rigid bodies within a chain. The objective of the project is to reach the two DOF of the prototype according to the design specifications defined above. Therefore, substituting $p = 2$ in (1), $n = 3$ is obtained; that is, a three cable-driven system is needed to reach the two DOF parallel mechanism.

2.2. *Mechanical System*

In section II.A it was determined that for the parallel mechanism to be develop in this work three cables are needed. Fig. 3 shows a general outline of the prototype to be designed.

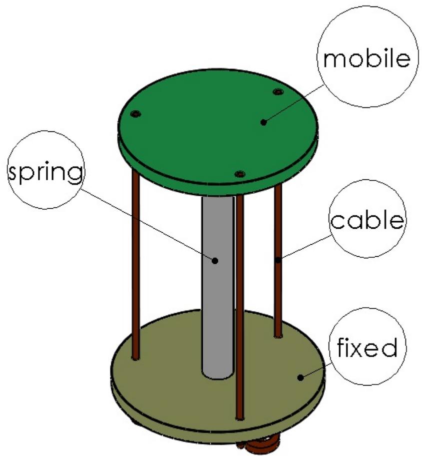

Figure 3: Sketch of the parallel mechanism.

A spring will be used as a central column, which must be suitably designed to provide the sufficient force required to maintain the tension in the cables and can buckle around the neutral axis to generate two DOF rotation. The material for the spring is ASTM A228 and the equation that describes the deflection of the spring can be approximated to:

$$\delta = \frac{8FD^3N_a}{Gd^4} \tag{2}$$

where δ is the compression deformation; D is the diameter of the spring (helix); d is the diameter of the wire; Na is the number of coils; G is the shearing modulus; E is the elastic modulus and F is the applied load of $1Kg$ as a design requirement. Table I presents the values of the parameters of the selected compressive spring.

Table 1: PARAMETERS OF SELECTED COMPRESSIVE SPRING

δ [m]	L_o[m]	d [m]	Na	F [N]	G [GPa]	E [GPa]
0,001	0.1	0.003	15	9,8	80	200

Solving for D from Equation (2) and replacing with the data of Table I, the spring diameter obtained is $D = 0.03m$.

Once the spring is designed, it is necessary to know the force to be applied by the mechanism to reach the desired angle of inclination. By deduction, the maximum force will be achieved when the mechanism reaches the maximum angle of inclination of the spring. The study of the force will be based on the static analysis (Gao et al. (2010)) of a mechanism with one DOF, inspired by the bending movement of the human neck.

According to our design specifications, the prototype will perform pitch and roll movements with a maximum angle of inclination of 40°. According to (Gao et al. (2010)) the buckling angle is proportional to the force input. With the help of Matlab Curve Fitting Tool, as shown in Fig. 4, we can find the curve linearly adjusted that relates the angle (input) vs. the cable tension (output), using the spring parameters in Table I and considering a load for the mobile platform of $1Kg$. The distance between the center of the base and each of the cables is $0.05m$.

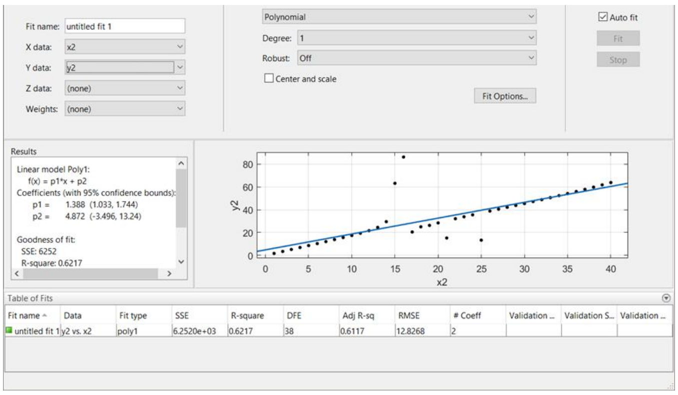

Figure 4: Angle (°) vs. tension (N)

The equation obtained for the adjustment curve is:

$$T = 1.338\theta_x - 4.872 \quad (3)$$

where T is the tension and θ_x is the inclination angle.

Replacing θ_x by 40°, that represents the angle of maximum design inclination, results in a tension of $60.392N$. Knowing this force it is possible to realize the sizing of the motors whose function will be to control the displacement of the cables of the CDPM mechanism.

2.3. Electrical System

At this step, it is necessary to know the nominal torque required for the motor when the mechanism reaches the maximum flexion angle of 40° and with an efficiency of 85%, considering the existence of friction between components. Equation (4) represents the transmission configuration by crane.

$$M = \frac{d_1}{2}\frac{T}{n} \quad (4)$$

where M is the force torque, T is cable tension calculated previously and n is the efficiency (85 %). Knowing that the diameter of the pulley is $d_1 = 0.02m$, the required torque M can be determined.

The result of Equation (4) is $M = 0.71Nm$. With the help of the Maxon selection program, the selected motor is RE 273757 with Planetary Gearhead 166155. For the control of the DC motor, the driver IPOS 4808 MX will be used through CAN communication.

2.4. Parallel Prototype

The CDPM mechanism is shown in Fig. 4, which represents the proposed prototype of soft robotic neck of two DOF.

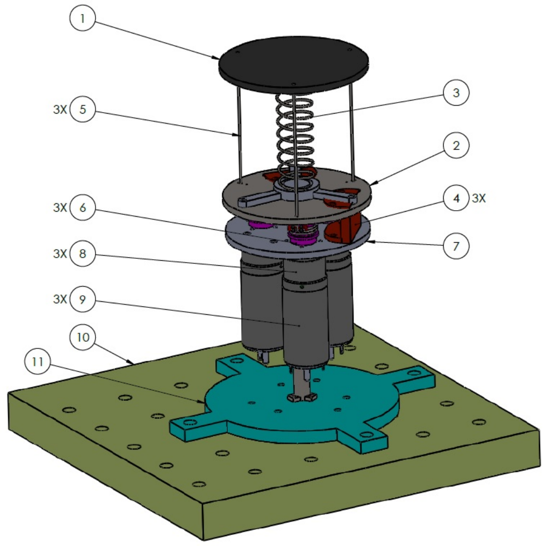

Figure 5: Prototype functional scheme.

Table II presents the different parts of the system and Table III shows the general specifications of the prototype.

A compressive spring serves as the main mechanical structure of the soft robotic neck. Element 2 (Table II) acts a a fixed base, while Element 1 (Table II) is a mobile platform driven by three symmetrically distributed cables that are pulled by the DC motors located below the fixed base.

3. Mathematical Model

The CDPM shown in Fig. 6 consists of: a fixed base, a moving platform, three flexible cables with negligible mas and a compression spring. The coordinate frame $OXYZ$ is attached to the fixed base and the Y-axis is along OA_1. The coordinate frame $oxyz$ is attached to the moving platform and the y-axis is

Table 2: ELEMENTS OF SOFT ROBOTIC NECK

	Element
1	Mobile Platform
2	Fixed Base
3	Spring
4	Pulley
5	Cable
6	Shaft Rotation
7	Motor Base
8	Planetary Gearhead
9	DC Motor
10	Platform
11	Mounting Base

Table 3: GENERAL SPECIFICATIONS OF THE PROTOTYPE

Technical specification	Value
Load capacity	1Kg
Degrees of freedom	2
Voltage	48V DC
Approximate weight	12.5Kg
Type of mechanism	CDPM
Approximate dimensions	0.11 x 0.11 x 0.262m
Tilt range	0°- 40°
Sensors	Encoders
Actuator	DC Motor: Maxon RE 273757

along OB_1. The moving platform is driven by three cables and the connection points are $\overrightarrow{oB} = (B_1; B_2; B_3)$; the other end of each cable connects to a roller driven by a motor and the cables pass through the fixed base at points $\overrightarrow{OA} = (A_1; A_2; A_3)$. We will denote the force value along the cable as T_i and the cable length between A_i and B_i as l_i.

In the plane formed by O, o and o', with o' the projection of o to the fixed base, a planar body frame Ost is attached to the spring, as show in Fig. 7. The origin is the same as the base coordinate frameOXZ, the t-axis is the same as the Z-axis and the s-axis is along Oo'.

As shown in Fig. 6 and Fig. 7, the configuration of the moving platform is defined by four parameters: θ_s is the angle between the s-axis and the X-axis; θ_p is the angle between the fixed base plane and the moving platform plane; t_0 is the vertical length of the bending spring; s_o is lateral translation of the bending spring. There are three parameters independent from each other, considering s_o as the dependent parameter. In other words, once θ_s, θ_p and t_0 are given, s_o can be solved. In this case, s_o is considered as a parasitic movement Carretero et al. (2000) that can be determined by the other three parameters.

Since θ_s and θ_p describe the orientation of the moving platform, using the Euler angles with orientation ZYZ the rotational matrix (5) can be obtained, which represents the projection from frame oxyz to $OXYZ$.

$$ {}^{O}R_{o'} = \begin{bmatrix} R_{11} & R_{12} & R_{13} \\ R_{21} & R_{22} & R_{23} \\ R_{31} & R_{32} & R_{33} \end{bmatrix} \tag{5} $$

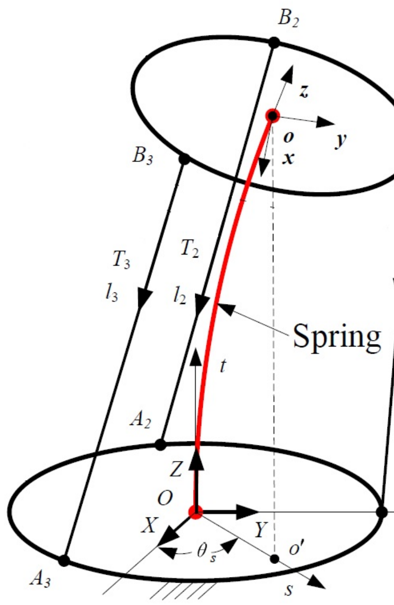

Figure 6: CDMP model.

where

$R_{11} = \sin^2\theta_s + \cos\theta_p \cos^2\theta_s$
$R_{12} = R_{21} = (\cos\theta_s - 1)\cos\theta_s \sin\theta_s$
$R_{13} = -R_{31} = \sin\theta_p \cos\theta_s$
$R_{22} = \cos^2\theta_s + \cos\theta_p \sin^2\theta_s$
$R_{23} = -R_{32} = \sin\theta_p \sin\theta_s$
$R_{33} = \cos\theta_p$

The homogeneous transformation matrix (6) from the moving coordinate frame to the base coordinate frame is:

$$ {}^{O}T_{o'} = \begin{bmatrix} {}^{O}R_{o'} & P_o \\ 0 & 1 \end{bmatrix} \tag{6} $$

where P_o is the position vector of point o with respect to the base coordinate frame, and $P_o = \begin{bmatrix} s_o\cos\theta_s & s_o\sin\theta_s & t_0 \end{bmatrix}^T$.

The procedure for the solution of the mathematical model (based on Gao et al. (2012)) of the soft robotic neck is represented in Fig. 8.

The inverse position kinematics problem is to calculate the cable lengths $L = \begin{bmatrix} L_1, & L_2, & L_3 \end{bmatrix}^T$given the desired moving platform posture $x = \begin{bmatrix} \theta_s & \theta_p & t_0 \end{bmatrix}^T$, which can be described as:

$$ L = f(x) \qquad f : \mathbb{R}^3 \longrightarrow \mathbb{R}^3 \tag{7} $$

The cable lengths are calculated by:

$$ L_i = \left\| {}^{O}T_{o'}\overrightarrow{oB_i} - \overrightarrow{OA_i} \right\| \quad (i = 1,2,3) \tag{8} $$

However, s_o cannot be an arbitrary number. We transform all the cable forces to two perpendicular forces F1 and F2 in the bending plane Ost, and a moment M perpendicular to the plane at the spring's top center, as shown in Fig. 7. The mass of the moving platform m is taken as a mass point at the spring's top center. The equilibrium conditions for force and torque at the

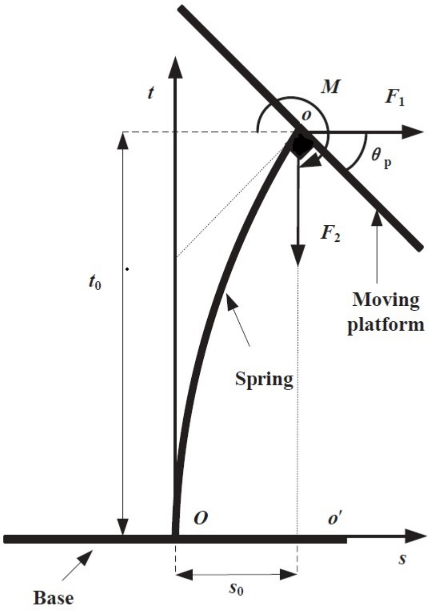

Figure 7: Lateral bending of the spring.

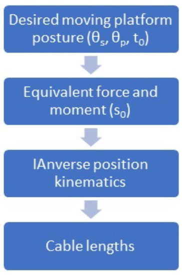

Figure 8: Solution of the soft neck mathematical model.

moving platform, as shown in Fig. 7, are as follows:

$$\sum_{i=1}^{3} {}^{O}T_i + F = 0 \tag{9}$$

$$\sum_{i=1}^{3} {}^{O}r_i \times {}^{O}T_i + M = 0 \tag{10}$$

where

$${}^{O}T_i = T_i({}^{O}T_{o'}\overrightarrow{oB_i} - \overrightarrow{OA_i}) / \left\| {}^{O}T_{o'}\overrightarrow{oB_i} - \overrightarrow{OA_i} \right\|$$

$${}^{O}r_i = {}^{O}R_{o'} \cdot \overrightarrow{oB_i}$$

$$F = \begin{bmatrix} -F_1 \cos\theta_s, & -F_1 \sin\theta_s, & F_2 - mg \end{bmatrix}^T$$

$$M = \begin{bmatrix} -M \sin\theta_s, & M \cos\theta_s, & 0 \end{bmatrix}^T$$

Considering β as the flexural rigidity after compression of the spring Timoshenko (1936), the lateral bending curve of the spring spine can be taken as the following linear equation Gao et al. (2013):

$$\beta \frac{d^2 s}{dt^2} = M + F_2(s_0 - s) + F_1(t_0 - t) \tag{11}$$

with initial conditions:

$$s(0) = 0,\ s'(0) = 0,\ s(t_0) = s_0\ s'(t_0) = \tan\theta_p \tag{12}$$

where $s' = ds/dt$. Using the spring bending equation (11) and (12), s_o can be obtained; therefore, the inverse position problem can be solved, as shown in the following section.

4. Simulation Results

To validate the design of the spring, a tension study is performed so as to check if, when applying the forces to reach the maximum flexion angle of 40°, the elastic limit of the spring is not overpassed. The elastic limit of the A228 steel is $2000Mpa$ for $d = 0.003m$. Fig. 9(a) shows how the spring acts as a central column and reaches a flexion of 40°, being able to recover its initial state since the elastic limit does not exceed the theoretical one. Fig. 9(b) shows that the maximum strain is suffered by the middle area of the spring.

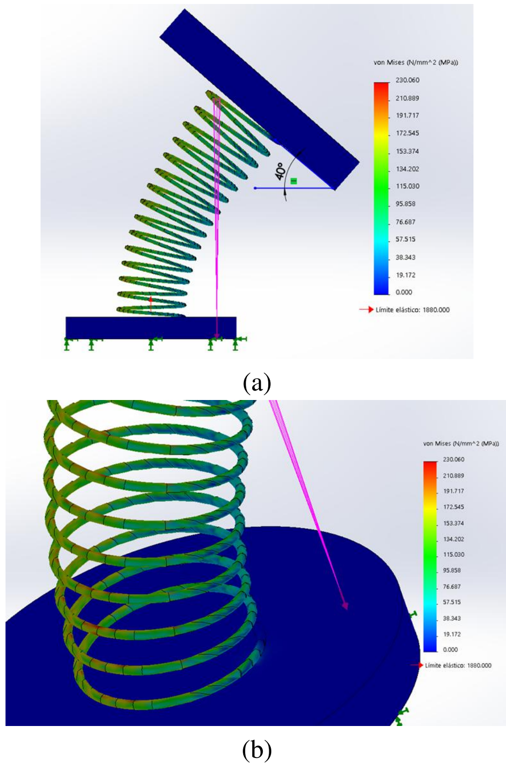

Figure 9: Simulation: (a) Tension study for spring validation, (b) Spring zone where maximum strain is applied.

Reverse kinematics and static analysis are implemented in Matlab. Additionally, the inertia I and bending constant β_o of the spring must be calculated with the following equations:

$$I = \frac{\pi d^4}{64}; \qquad \beta_o = \frac{2EGIL_0}{\pi N_a \frac{d}{2}(E + 2G)} \tag{13}$$

whose constants values are given in Table I. The implementation is performed with a fixed $t_o = 0.085m$, varying θ_p from 0° to 40° and θ_s from 0° to 360°. We can obtain the results shown in Fig. 10, where the cable lenghts corresponding to each set of thetap and thetas are represented in the z-axis.

In Fig. 10, it is observed that while θ_p is large, the variation in cable length is also large. This is because the more the mobile base is tilted, the greater amount of force will be required.

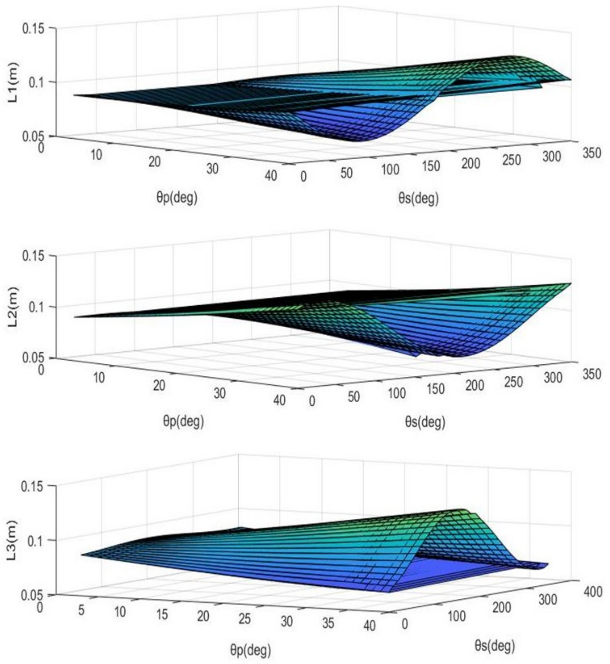

Figure 10: Inverse position kinematics.

5. Conclusions

This paper has presented the design of a soft robotic neck with two DOF providing pitch and roll movements. The constraints are a maximum inclination of 40° and a maximum load for the neck of $1Kg$. The mechanical and electrical design of the prototype have been addressed taking these constraints into account. The mechanism uses a coil compression spring to simulate the cervical vertebrae and cables that act as muscles.

The cables of the mechanism are tensionable everywhere and can be rigidified only by a large spine. This fact, reduces the inertia of the manipulator, which is desirable in many applications, including high-speed robotics.

The mathematical model of the neck has been presented and the theoretical static analysis of the mechanism has been performed. The simulation results clearly show that the performance of the system allows the spring column to perform within its elastic range.

Future research steps will focus on the implementation of the real platform and its control strategy.

Acknowlegments

The research leading to these results has received funding from the HUMASOFT project, with reference DPI2016-75330-P, funded by the Spanish Ministry of Economy and Competitiveness.

References

Alfayad, S., El Asswad, M., Abdellatif, A., Ouezdou, F. B., Blanchard, A., Beaussé, N., Gaussier, P., 2016. Hydroïd humanoid robot head with perception and emotion capabilities: Modeling, design, and experimental results. Frontiers in Robotics and AI 3, 15.

Behzadipour, S., Khajepour, A., 2006. Cable-based robot manipulators with translational degrees of freedom. En: Industrial Robotics: Theory, Modelling and Control. InTech, pp. 221–236.

Beira, R., Lopes, M., Praça, M., Santos-Victor, J., Bernardino, A., Metta, G., Becchi, F., Saltarén, R., 2006. Design of the robot-cub (icub) head. En: Robotics and Automation, 2006. ICRA 2006. Proceedings 2006 IEEE International Conference on. IEEE, pp. 94–100.

Carretero, J., Podhorodeski, R., Nahon, M., Gosselin, C. M., 2000. Kinematic analysis and optimization of a new three degree-of-freedom spatial parallel manipulator. Journal of mechanical design 122 (1), 17–24.

Gao, B., Song, H., Sun, L., Tang, Y., May 2013. Inverse kinematics and workspace analysis of a bio-inspired flexible parallel robot. En: 2013 IEEE International Conference on Cyber Technology in Automation, Control and Intelligent Systems. pp. 138–143.
DOI: 10.1109/CYBER.2013.6705434

Gao, B., Xi, N., Shen, Y., Zhao, J., Yang, R., 2010. Development of a low motion-noise humanoid neck: Statics analysis and experimental validation. En: Robotics and Automation (ICRA), 2010 IEEE International Conference on. IEEE, pp. 1203–1208.

Gao, B., Xu, J., Zhao, J., Xi, N., 2012. Combined inverse kinematic and static analysis and optimal design of a cable-driven mechanism with a spring spine. Advanced Robotics 26 (8-9), 923–946.
URL: http://www.tandfonline.com/doi/abs/10.1163/156855312X633048
DOI: 10.1163/156855312X633048

Gao, B., Zhao, J., Xi, N., Xu, J., 2011. Combined kinematic and static analysis of a cable-driven manipulator with a spring spine. En: Robotics and Automation (ICRA), 2011 IEEE International Conference on. IEEE, pp. 2725–2730.

Gosselin, C., June, 15, 1988. Kinematic analysis, optimization and programming of parallel robotic manipulators. McGill University Montréal, Canada.

Han, J., Zeng, S., Tham, K., Badgero, M., Weng, J., 2002. Dav: A humanoid robot platform for autonomous mental development. En: Development and learning, 2002. Proceedings. The 2nd international conference on. IEEE, pp. 73–81.

Hashimoto, T., Hitramatsu, S., Tsuji, T., Kobayashi, H., 2006. Development of the face robot saya for rich facial expressions. En: SICE-ICASE, 2006. International Joint Conference. IEEE, pp. 5423–5428.

Hirukawa, H., Kanehiro, F., Kaneko, K., Kajita, S., Fujiwara, K., Kawai, Y., Tomita, F., Hirai, S., Tanie, K., Isozumi, T., et al., 2004. Humanoid robotics platforms developed in hrp. Robotics and Autonomous Systems 48 (4), 165–175.

Sakagami, Y., Watanabe, R., Aoyama, C., Matsunaga, S., Higaki, N., Fujimura, K., 2002. The intelligent asimo: System overview and integration. En: Intelligent Robots and Systems, 2002. IEEE/RSJ International Conference on. Vol. 3. IEEE, pp. 2478–2483.

Tadesse, Y., Subbarao, K., Priya, S., 2010. Realizing a humanoid neck with serial chain four-bar mechanism. Journal of Intelligent Material Systems and Structures 21 (12), 1169–1191.

Timoshenko, S., 1936. Theory of elastic stability, 1st Edición. New York McGraw-Hill Book Company, inc, bibliographical foot-notes.
URL: http://openlibrary.org/books/OL24757780M